Eur. Phys. J. D (2015) 69: 23
DOI: 10.1140/epjd/e2014-50313-2

THE EUROPEAN PHYSICAL JOURNAL D

Regular Article

Evaluation of plasma density in RF CCP discharges from ion current to Langmuir probe: experiment and numerical simulation*

Dmitry Voloshin[a], Alexander Kovalev, Yuri Mankelevich, Olga Proshina, Tatyana Rakhimova, and Anna Vasilieva

Skobeltsyn Institute of Nuclear Physics Lomonosov Moscow State University (SINP MSU), 1(2), Leninskie gory, 119991 Moscow, Russian Federation

Received 18 April 2014 / Received in final form 5 September 2014
Published online 21 January 2015 – © EDP Sciences, Società Italiana di Fisica, Springer-Verlag 2015

Abstract. Experimental measurements of current-voltage relationship in RF CCP discharge in argon at 81 MHz have been performed by cylindrical Langmuir probes technique. Two different probe radii have been used: 50 and 250 μm. The high plasma density 10^{10}–10^{11} cm^{-3} has been estimated at specific input power under study. The experimental data on nonmonotonic behavior of probe current with pressure were observed firstly for conditions of RF discharge plasmas. To analyze the probe measurements the fast numerical model for ion current collected by a cylindrical probe has been developed. This model is based on the particle-in-cell with Monte-Carlo collision method for ions motion and Boltzmann relation for electrons. The features of probe data at studied conditions were discussed. The comparative analysis of different collisionless approaches for plasma density calculation from ion probe current is done. It is shown that in general collisionless theories underestimate the plasma density value. For correct evaluation of plasma density experimental I-V probe measurement should be supplied by the numerical simulation. It was demonstrated that the collisionless analytical theory of orbital motion can formally give correct results on plasma density at some plasma conditions even when ion collisions take place. The physical reasons of this accidental validity are explained.

1 Introduction

Probe measurements are fundamental plasma diagnostic methods. It allows determining the plasma parameters: plasma density, electron temperature and electron energy distribution function from probe I-V curve. Recently, probe measurements were used together with optical-emission and absorption spectroscopy to measure density of metastable and resonantly excited atoms with reasonable accuracy [1–4].

Current-voltage characteristics (I-V curve) obtained from the probe current can be divided roughly into two, ion and electron, parts. Determination of plasma parameters from the electron part of I-V curve is well established [5].

Evaluation of electron density on the basis of the electron part of I-V curves can be done by measurements of the electron current to a probe $I_p^e(V_{pl})$ when probe voltage is equal to the plasma potential or by integration of the electron energy distribution function (EEDF), namely the integration of the second derivative of I-V curve. Even a small error in I-V curve measurement can lead to the enormous distortion in EEDF. The low energy range ($\varepsilon_e < \bar{\varepsilon}_e$, $\bar{\varepsilon}_e$ is a mean electron energy) of EEDF contains the majority of electrons and provides the main contribution to the electron density calculation. To avoid the distortions of the low energy part of EEDF a small enough probe size and resistance of probe electric circuit are necessary. Careful RF compensation and filtration of main and higher harmonics of plasma oscillation in the probe current are very important [6], because a small error in plasma potential measurements leads to a high error in the electron current $I_p^e(V_{pl})$.

The level of ion probe current is much smaller than the electron current and the requirements to the probe's electric circuit are much less strict. It is especially important that the requirements for RF compensation and filtration of plasma oscillation harmonics are significantly weaker. At the same time the electron temperature can be obtained directly from the I-V curve of uncompensated Langmuir probe without calculation of second derivative [7]. It leads to the more reliable measurements of the ion part of I-V curve. Also in case of an electro negative discharge, when the negative ion density is much higher than the electron density, the usage of ion part can be the only option for determination of plasma density. However, the evaluation of plasma density from the ion part of I-V curve is not straightforward.

* Supplementary material in the form of one xls file available from the Journal web page at
http://dx.doi.org/10.1140/epjd/e2014-50313-2

[a] e-mail: dvoloshin@mics.msu.su

Mostly the analysis of experimental data on ion current is carried out on the base of collisionless or collision analytical theories. However the applicability of these theories decreases with plasma density and gas pressure. As a result, the development and application of a rather simple method for plasma density estimation are still a challenge.

The analytical theories for analysis of probe current-voltage characteristics were developed for different plasma conditions. Two main approaches for ion motion treatment in collisionless case are the orbital and radial ion motion theories. The original orbital motion limited (OML) theory was proposed by Mott-Smith and Langmuir in reference [8]. It assumes a large sheath such that the probe radius is much smaller than Debye length. OML theory was further developed in reference [9] for a finite sheath and monoenergetic ions and in reference [10] for Maxwellian ion energy distribution, which requires extensive computations (so called Bernstein-Rabinowitz-Laframboise (BRL) theory). The ion current on the cylindrical probe surface in this theory can be expressed in the simplest case ($T_e \gg T_i$, $V \gg T_+$) in the form:

$$I_P^{OML} = \frac{\sqrt{2} S_P e N_+}{\pi \sqrt{M_i}} \sqrt{eV}, \quad (1)$$

where S_p – is the probe surface area, e – elementary charge, N_+ – ion density, M_i – ion mass, V – potential difference between probe and plasma. In case of ion collection with $T_i \ll T_e$, the condition for OML theory applicability in terms of Debye number $D_\lambda = R_P/\lambda_D$ (R_p – probe radius and λ_D – Debye length) is $D_\lambda \leqslant 3$. This condition was derived from the particles trajectories calculation in reference [10]. For the plasma density values in the range 10^{10}–10^{11} cm^{-3} this criterion will be satisfied for the probes with radius less than 80 μm.

The radial ion motion theory was described in reference [11], the so called "cold ion theory of Allen-Boyd-Reynolds" (ABR). It assumes a large radius of the probe and thin sheath such that the ion motion is radial. In order to find the plasma density according to the ABR theory the differential equation

$$\frac{1}{r}\frac{\partial}{\partial r}\left(r\frac{\partial V}{\partial r}\right) = 4\pi e\left(\frac{I}{2\pi r l e\sqrt{\frac{2eV}{M_i}}} - N_0 \exp\left(-\frac{eV}{kT_e}\right)\right) \quad (2)$$

for spatial distribution of electric field potential was solved iteratively. I – is the ion current to the probe, when probe voltage is V_p. The plasma density N_0 was changed in each iteration, so that the value of the electric field potential on the probe surface obtained from (2) was equal to the given value of probe voltage V_p.

These commonly used collisionless theories of orbital and radial ion motion can lead to the wrong results if they are used for the estimation of plasma density in discharge conditions when ion collisions in the probe sheath and presheath area take place. The addition of ion collisions in the probe analytic theories was done in references [12,13] to describe the ion current decrease due to the ion scattering. It was shown in reference [14] that ion collisions affect the probe current in a twofold way. The small number of collisions increases the ion current due to destruction of orbital motion, but with further increase in pressure the probe current decreases due to the ion collision "drag force". The collision theory [15] incorporates the probe current increase theory [14] and the theory [12,13] of current decrease due to ion scattering. The effect of ion collisions on current to the cylindrical and spherical probes was also studied in reference [16]. As a result the correction factor to the ABR theory current was introduced in the specific range of ion collision frequency. Nevertheless, these collision analytic theories are not widespread, possibly due to a large number of the involved approximations and assumptions. Up to date the standard I-V curve interpretation program of Hiden Analytical probe allows choosing of one of the described collisionless theories for density evaluation [17]. Collision theories are also out of the scope and OML formula is recommended for plasma density evaluation in recent paper [18] on probe data interpretation.

Fast growth of available computation resources allows implementing numerical physical models with less simplification. Kinetic simulation of probe current collection was done in references [19–22]. In reference [19], the ion motion was studied in the predetermined spatial potential profile. The twofold role of ion collisions was illustrated in the ion path figure in paper [20]. The experimental results on Ar^+ ion motion in helium [23] was used in reference [20] for comparison with the simulation results. The increase of ion collisions influence on I-V curve in case of Ar^+ motion in argon due to the resonance charge exchange collisions is pointed out in reference [20]. In reference [21], both electrons and ions were treated kinetically in the self-consistent electric field, but the plasma densities of 10^7–10^8 cm^{-3} were significantly less than the density values in the plasma processing. In reference [22], the I-V curve variation with pressure is shown for a fixed plasma density of 10^9 cm^{-3}.

However the plasma density can reach the value of 10^{10}–10^{11} cm^{-3} in modern plasma processing reactors. This paper expands kinetic study of ion current to the probe for these high plasma densities and for the CCP discharge parameters typical for plasma processing (i.e., for argon pressures from 1 to 200 mTorr). In our study, for the first time the kinetic simulation of Ar^+ ion motion in Ar is presented together with the experimental measurements of I-V curve in argon for typical plasma processing conditions. I-V curves in RF CCP discharge at 81 MHz frequency have been measured at an argon gas pressure up to 200 mTorr and a specific input power up to ~0.4 W/cm^2. The Probe model with the kinetic treatment of ions motion based on Particle in cell with Monte-Carlo collisions (PIC MCC) method and different approaches for electrons motion was developed to estimate the plasma density from the measured I-V curve. The probe simulation results were compared with the data on I-V curves processing with using of the different analytical approaches. Also the self-consistent PIC MCC discharge simulation was done to test the discharge parameters and the Probe model input data.

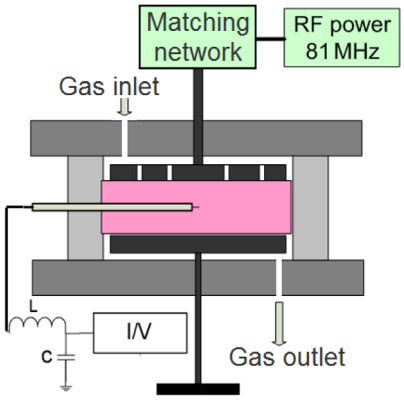

Fig. 1. Scheme of the experimental setup.

The present study focuses on the measurements and calculations of the ions currents on the cylindrical probes of different radii, and seeks to establish the correct procedure of plasma density determination in a wide range of the gas pressures and plasma conditions.

This paper is organized as follows. In the next section, the experimental setup scheme and results are presented. In Section 3, the numerical model is described with the analysis of plasma modeling approaches. In Section 4, the comparative analysis of different methods for I-V curve processing are presented. The role of ion collisions is discussed. It is shown that collisionless OML theory gives the plasma density values close to the values from numerical model in some range of parameters. This can lead to the wrong conclusion about applicability of this theory. Section 5 ends the paper with final recommendations and conclusions.

2 Experiment

Experimental measurements of current-voltage relationship in 81 MHz CCP discharge in argon were performed by using of cylindrical Langmuir probes of two different radii: 50 and 250 μm. 81 MHz RF frequency was chosen for discharge excitation because of the wide plasma bulk region and EEDF close to Maxwellian one at this frequency in CCP discharge in our simulation. The discharge parameters were varied in the following range: neutral gas pressure 30–200 mTorr, input power 5–30 W, estimated plasma density: 10^{10}–10^{11} cm^{-3}. The usage of two probes with different radii allows us to validate the OML theory predictions on the proportionality of the probe ion current to the probe radius.

The scheme of the experimental setup is shown in Figure 1. The inner diameter of the quartz discharge tube is 100 mm. The distance between two duralumin electrodes (95 mm in diameter) is $d = 30$ mm. Gas inlet is mounted in the top electrode. Gas was fed through 60 holes 0.5 mm in diameter in electrode. The exhaust was led out through the bottom electrode. The bottom electrode was grounded, and the RF power was applied to the top electrode by the matching network. The 81 MHz RF generator of the power up to 30 W was used on these experiments. The power loading to the electrode is up to 0.38 W/cm^2 which corresponds to the real plasma processing chambers. The RF power dissipated in the discharge, i.e. the input RF power, was measured by bi-directional power-meters of forward and reflected waves before matching network. Losses in the matching network have been determined by the method used by Horwitz [24] and by Godyak and Piejak [25]. It was obtained that power losses weakly depend on the input power and strongly depend on the gas pressure. The values of power losses are 15% for a pressure of 200 mTorr, 22% for 100 mTorr and 32% for 30 mTorr.

Plasma was confined in the interelectrode gap by the grids that prevent the plasma penetration into the gap between electrodes and quarts chamber walls.

Molybdenum probes with two different radii of 50 and 250 μm and with a length of 9 mm were used in the experiment. The probe could be moved both along the interelectrode gap and along the radius of the discharge chamber. For high-frequency voltage compensation the LC filter was used. To check the adequateness of RF filtration (and also the very weak dependence of obtained plasma potential value from this filtration) the I-V curve was measured for different parameters of LC filter. The inductance L was changed from 0 up to 500 μH. Ion part of I-V curves can not be distinguished between each other starting from $L = 36$ μH. Self-capacitance of the LC filter does not increase from the $L = 36$ μH, because L was added with series connection. And up to 36 μH, the coils with low transfer capacitance was used. The reference electrode was not used, because there is no need in it when the electron density is measured by the ion part of I-V curve [7]. The probe measurement unit consists of the amplifier for probe voltage and the isolated (separate) amplifier of probe current. The automated data acquisition and processing system was used. The output voltage of probe scheme was measured by National Instruments DAQ card. The probe voltage could be changed in a range from –150 V to 150 V. The electron temperature T_e on the assumption of Maxwell EEDF was calculated from I-V curve slope in the semi logarithmic scale. There was a long part of I-V curve with a linear dependence on the voltage logarithm. The plasma potential was determined from the zero second derivative of the probe current on the probe potential. The plasma potential values are shown in Figure 2 for the range of the neutral gas pressure and input power.

These values of plasma potential are in a good agreement with the experimentally measured peak of the ion energy distribution function (IEDF) in case of 81 MHz discharge [26]. The IEDF at the ground electrode are shown in Figure 3 for neutral gas pressure of 30 mTorr and input power of 10 W. The plasma potential value uncertainty within 5 eV does not change the results on plasma density of our Probe model simulation. This is because the ion part of I-V curve at high probe voltages is quite flat.

The Langmuir probe was immersed in plasma under a potential of –70 V between the measurements and was cleared due to ions impact. Also it was cleared periodically

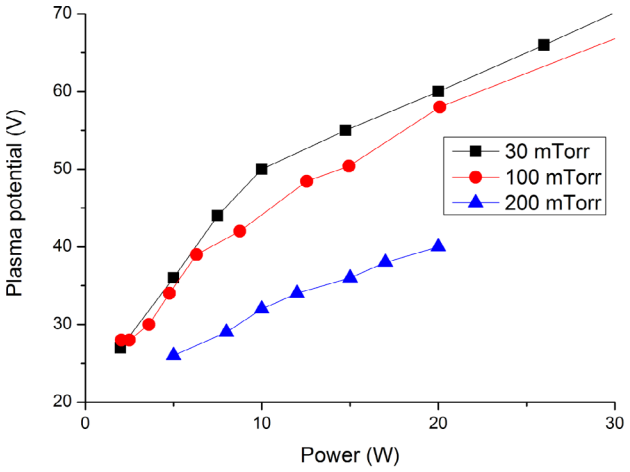

Fig. 2. Plasma potentials derived from the measured *I-V* curves for a range of input powers and three different gas pressures.

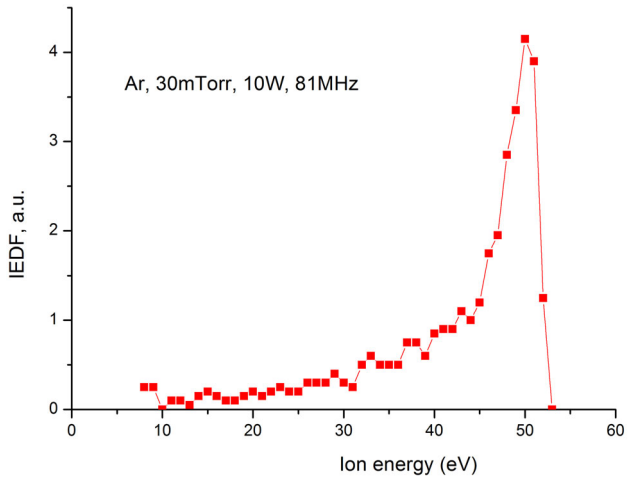

Fig. 3. IEDF at the ground electrode. Pressure 30 mTorr, input power 10 W.

in oxygen plasma and the difference in the measurements before and after clearing was monitored.

The typical experimental *I-V* curves obtained with two probes of 50 and 250 μm radius are shown in Figure 4 for different values of input power at a neutral gas pressure of 30 mTorr. The *I-V* curves for pressures of 100 and 200 mTorr for both probe radii can be found in the Supplementary data* to this paper. The electron part of *I-V* curve is shown in the separate window in the figure since the electron current absolute value is much greater than the ion current value.

3 Simulation

To reveal the effect of ion collisions on the probe current value, the kinetic methods for description of the ions motion should be used.

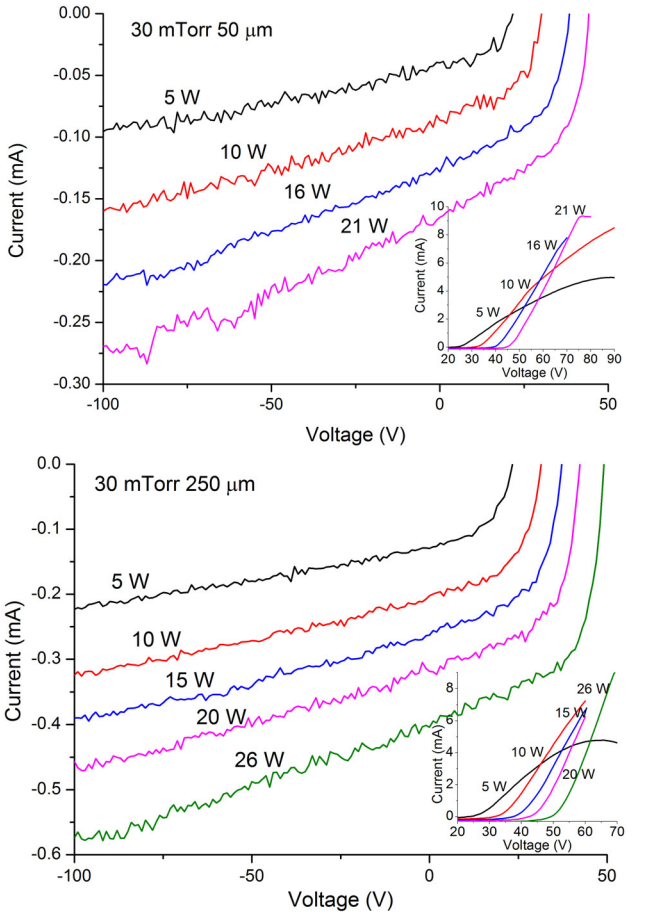

Fig. 4. *I-V* curve for 30 mTorr pressure and several values of input powers. Probe radius (a) 50 μm and (b) 250 μm.

The ion motion is treated kinetically via PIC MCC model. Ions elastic and charge exchange collisions with Ar atoms are included in the model with the cross sections from paper [27] for these processes. The ion elastic scattering is isotropic in the center of mass system. For the charge exchange collisions, ion losses all its energy and gets the thermal energy of Ar atom. The grid is uniform with a cell size less than or equal to the Debye length, depending on the statistic. The maximum number of super particles was set to be 1.5×10^5. To avoid a statistical noise near the smallest radial grid points the weighting scheme with variable weight $w_p \sim 2\pi r dr$ was used. Numerical convergence tests were performed to check numerical errors. The simulation without the probe was done to ensure that the average particle energy is not changed in time during the simulation and that the variable weights of the particles do not produce any numerical errors.

The ion flux from the undisturbed plasma (thermal ion flux in the plasma bulk) $N_0 v_{ion}$ was set on the outer boundary $r = r_{\max}$. Here N_0 – is the plasma density, v_{ion} – is the ion velocity corresponds to the ion thermal energy $T_i = 0.026$ eV. During one time step $(2\pi r_{\max} N_0 v_{ion} dt/w_p)$ of superpaticles can be born. The velocity of new superparticle at the r_{max} boundary is chosen randomly in amplitude according to the spatially isotropic Maxwellian

distribution with $T_i = 0.026$ eV. Only the superparticles with the velocity directed to the simulation region are added to the simulation. The ions are absorbed by the probe at $r = r_{probe}$.

The value for maximum radial distance from the probe $r_{\max}$ is chosen to include both sheath and presheath regions. The ion flux out of the simulation area through outer boundary $r_{\max}$ is non-zero in this case. The size of the Probe model region (that is probe sheath and presheath area) can be compared with the ion mean free path length $\lambda_{Ion} = 1/(330 \times p$ [Torr]). For the pressures of 30–200 mTorr under study the λ_{Ion} values are 0.1–0.015 cm, respectively. The $r_{\max}$ value in our simulation is in a range of 0.15–0.5 cm depending on the gas pressure and the plasma density. As a result, ions undergo collisions before reaching the probe surface for all experimental regimes under study. Therefore the collisionless theories for ion current to the probe can provide wrong results in plasma density values.

One can apply a kinetic treatment like PIC MCC for both electrons and ions motion [21]. The simulation of the whole I-V curve with the ion and electron part is possible in this case.

However as it was pointed out in reference [22] such approach can be inappropriate if the ionization collisions take place in the simulation area of the probe sheath and presheath. The balance of the ionization and the particle loss on the probe surface (volume loss through recombination is negligible in our conditions) is broken in this case. This leads to the equilibrium plasma density that differs from that of initial undisturbed plasma. Besides that, if electrons are treated as particles in simulation process, they only loose their energy in collisions and do not gain the energy from the applied electric field (only the electric fields induced by the probe and charged particles are simulated). So in these conditions the electrons are assumed to be in equilibrium with electric field according to Boltzmann relation: electron density distribution is determined by the plasma potential distribution $N_e(r) = N_0 \exp(-e\phi(r)/kT_e)$. Here N_0 – plasma density, $\varphi(r)$ – potential profile, T_e – electron temperature.

Both approaches for electrons treatment described above were implemented in our models. The limiting value of gas pressure for applicability of PIC method for electrons was estimated. Namely, assuming Maxwellian electron energy distribution function it is possible to find the ionization coefficient $\langle\sigma v\rangle^{ioniz}$ for the given T_e value. The cross sections for electron collisions with Ar atoms were taken from [28]. The effective "ionization current" $I^{ioniz} = eR_iV$, where ionization rate $R_i = \langle\sigma v\rangle^{ioniz} NN_e$ and simulation volume $V = \pi r_{\max}^2 l_{probe}$, can be compared with the ion probe current I^{probe}. Here N – neutral atom density, N_e – plasma density (10^{10} cm^{-3} for the upper bound pressure value) and l_{probe} – is the probe length (0.9 cm). The treatment of electrons motion with PIC method could be applicable if the effective "ionization current" is smaller than typical current to the probe in the conditions under study: $I^{ioniz} \ll I^{probe}$. This inequality holds for pressure values less than 10 mTorr with

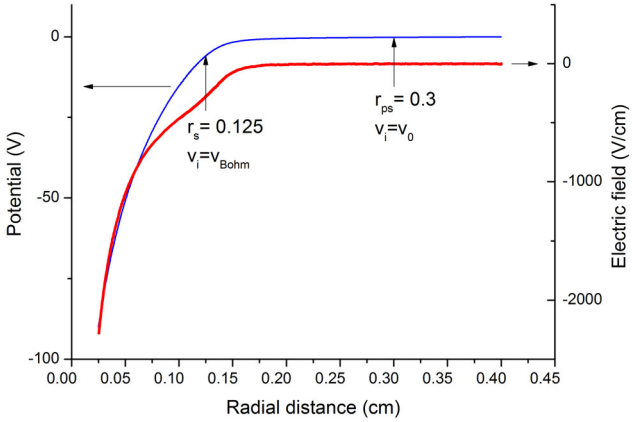

Fig. 5. Spatial distribution of potential and electric field in the simulation. Discharge parameters $p = 100$ mTorr, $r_p = 250$ μm, $N_0 = 10^{10}$ cm^{-3}, $\phi_{probe} = -90$ V, $\phi_{plasma} = 0$ V.

$I^{ioniz} = 0.074$ mA, $I_{50}^{probe} = 0.075$ mA, $I_{250}^{probe} = 0.117$ mA at $p = 10$ mTorr (with subscript index denoting probe radius in micrometers). As the experimental pressures were higher than 10 mTorr the Boltzmann relation for electron has been used for modeling the experimental I-V curves.

In the Probe model, one dimensional Poisson equation is also solved numerically in cylindrical geometry. The distribution of the electric field obtained in the simulation is shown in Figure 5. The following boundary conditions were used for Poisson equation. The electric field potential $V(r_{\max})$ is always set to zero for computational convenience. The boundary condition at the probe surface is $(V_p + V_{bias})$ which is the sum of the real plasma potential and the probe bias. The measured plasma potential values shown in Figure 2 were used in the simulation. The Poisson equation becomes non-linear in case of Boltzmann relation for electron concentration and is solved by the iterative Newton-Raphson method [29].

The following input parameters were used in the model: argon gas pressure p, plasma potential ϕ_{plasma}, electron temperature T_e, and varying plasma density N_0. For this set of input parameters the Probe model provides the ion probe current I_P.

Also the self-consistent PIC MCC discharge simulations [26,30] were carried out to calculate the discharge parameters and to verify additionally input data taken from the experimental measurements and the Probe model assumptions (the EEDF shape, the value of electron temperature T_e and the spatial profile of plasma density – the width of the bulk comparing to the width of the probe sheath and presheath region).

The electron temperature estimated from the experimental I-V curves was varied in the range 2.5 ± 0.5 eV for various input powers and neutral gas pressures. The PIC simulations of CCP discharge in similar discharge conditions also resulted in the values of T_e close to 2.5 eV. So $T_e = 2.5$ eV was used in all simulations of the ion probe currents. We also check the sensitivity of the plasma density obtained in our Probe model to the variation of T_e. The simulations with T_e equal to 2 and 3 eV show the

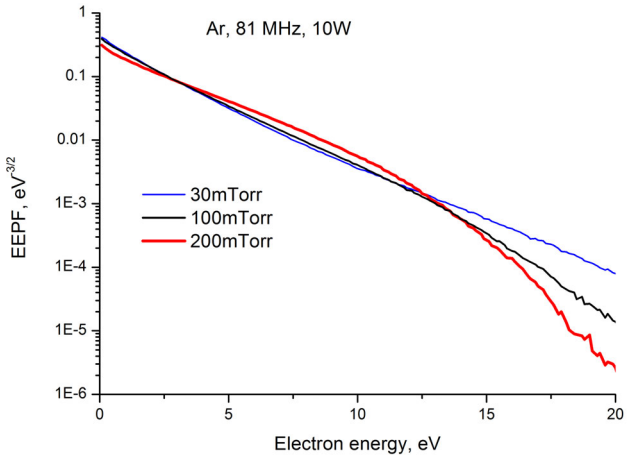

Fig. 6. Electron energy probability function in center of the discharge. Results of PIC MCC simulation.

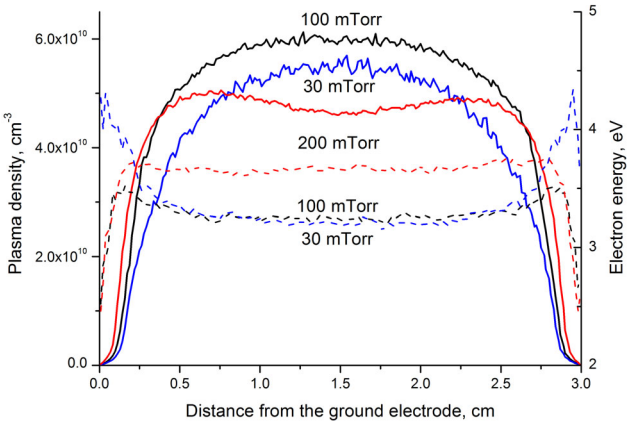

Fig. 7. Spatial distribution of plasma density and average electron energy in the discharge gap. Results of PIC MCC simulation for input power of 10 W.

decrease and increase of plasma density within 10% from the density for $T_e = 2.5$ eV.

The EEPF in the center of the discharge, obtained in the self-consistent PIC MCC simulation is shown in Figure 6 for three pressures studied experimentally in this work: 30, 100, and 200 mTorr. One can see that these EEPFs are close to Maxwellian ones up to ∼14 eV.

The estimated $r_{\max}$ value can be also compared with the plasma bulk width obtained from the time-averaged spatial distribution of plasma density and the average electron energy between electrodes in the self-consistence PIC MCC discharge simulation. These distributions are shown in Figure 7 for input power of 10 W.

The bulk region is the smallest one in the case of 30 mTorr discharge. The $r_{\max}$ value from Probe model is smaller than 0.5 cm for the lowest plasma density of 10^{10} cm^{-3}. Even for this "worst" combination of bulk width and simulation area, the probe sheath and presheath region is located entirely in the plasma bulk region with the near constant plasma density as it is seen from Figure 7. This confirms the assumption of a constant plasma density and zero averaged electric field in the undisturbed region in our Probe model. The $r_{\max}$ drops with plasma density and the plasma bulk width is increased with pressure.

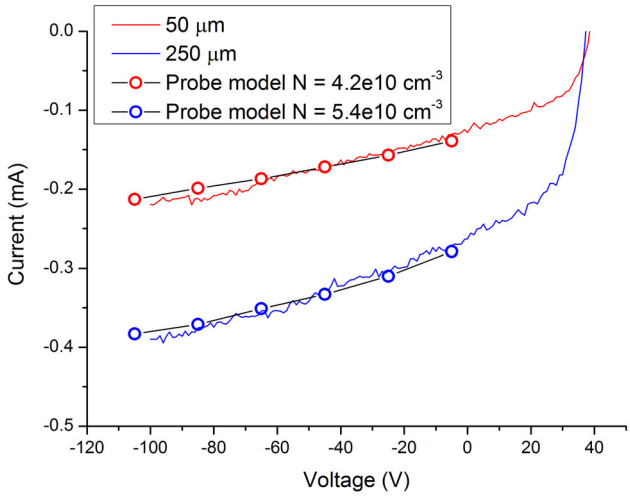

Fig. 8. I-V curves fitting by Probe model with proper plasma densities for two probes ($r_p = 50$ and 250 μm, $p = 30$ mTorr and input power of 15 W).

The plasma density value N_0 is varied in our simulations until the calculated I-V curve becomes close to the measured one. The result of this procedure for $p = 30$ mTorr and input power of 15 W is shown in Figure 8. The plasma densities, estimated from I-V curve fitting and shown in the figure legend, are different for two probes.

This difference in plasma density drops with pressure in our simulation and is less than 20% for $p = 100$ mTorr and 10% for $p = 200$ mTorr. The unique value of plasma density should be independent from probe radius. We suppose the possible reason of the calculated plasma density nonuniqueness is the one-dimensional treatment of the electric field distribution. This issue will be studied with 2D electric field model. At high pressures, the possibly important effects of 2D electric field distribution could be neutralized by particle collisions and the Probe model results in the unique value of plasma density for both probe radii. As the plasma density nonuniqueness is vanished with pressure, we can apply the Probe model in present one-dimensional form (1D Probe model) for the study of the ion collisions effects.

The numerical simulation with the developed Probe model is quite fast. On the desktop computer with Intel core i7-3770s CPU, the one point of I-V curve is calculated for less than 10 s in the single thread mode. The precise time depends on the plasma density for which the ion current is calculated. So the Probe model can be applied to pre-calculate the I-V curves for different plasma densities under various experimental conditions and then to use these data for the real time analysis of the experimental I-V probe characteristics.

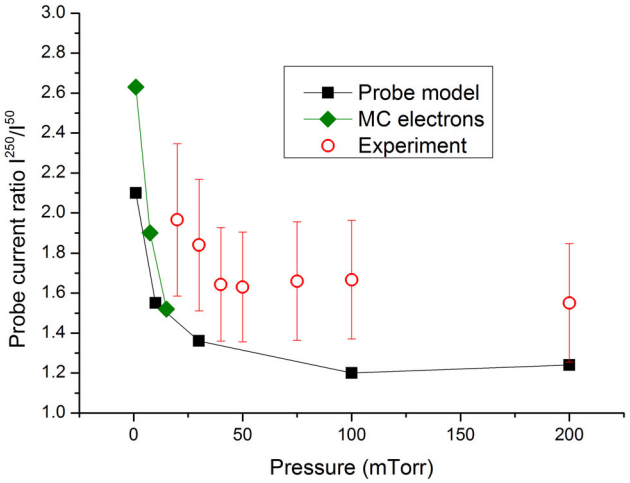

Fig. 9. Probe current ratio for probe radius 250 and 50 μm. I_P^{250}/I_P^{50}. Experimental data are for input power of 10 W. Calculated results are for plasma density of 10^{10} cm^{-3}.

4 Comparative analysis of the various approaches for I-V curve treatment and discussion

The collisionless analytic theories are often used for the interpretation of the ion part of I-V curves and calculation of the plasma density values even in collision conditions.

The condition for OML theory applicability $D_\lambda \leqslant 3$ [10] can be additionally tested with the help of two probes of different radii. The ratio of the ion probe currents was calculated for different discharge and probe parameters. According to OML theory formula (1) the probe current is proportional to the probe radius. The probe current ratio should be close to 5 if OML theory is correct in our case simultaneously for both probes with $r_p = 50$ and 250 μm.

The $D_\lambda = 3$ is realized in our discharge conditions for $r_p = 250$ μm and plasma density of 10^{10} cm^{-3}, so OML applicability in this boundary D_λ value can be checked. The probe current ratio as a function of pressure is shown in Figure 9. The curve labeled "MC e" in this figure shows the results of the simulation with PIC MCC electrons, which is possible for pressure lower than 10 mTorr as described previously. As it seen both the experiment and simulation show that OML regime does not occur simultaneously for both probes in the whole range of pressures from the collisionless ion motion at 1 mTorr to the collisional case at 200 mTorr. The slightly different shapes of the experimental and numerical results are due to fact that experimental data are obtained for a fixed power value of 10 W and the simulation data are obtained for a fixed plasma density of 10^{10} cm^{-3}.

The D_λ drops with the plasma density decrease. For plasma density of 10^9 cm^{-3}, the Debye length increases and the simulation shows the ratio of the currents for two probes close to the radii ratio. The simulations with two probe radii 10 μm and 50 μm and plasma density of 10^{10} cm^{-3} also shows OML regime for ion collection.

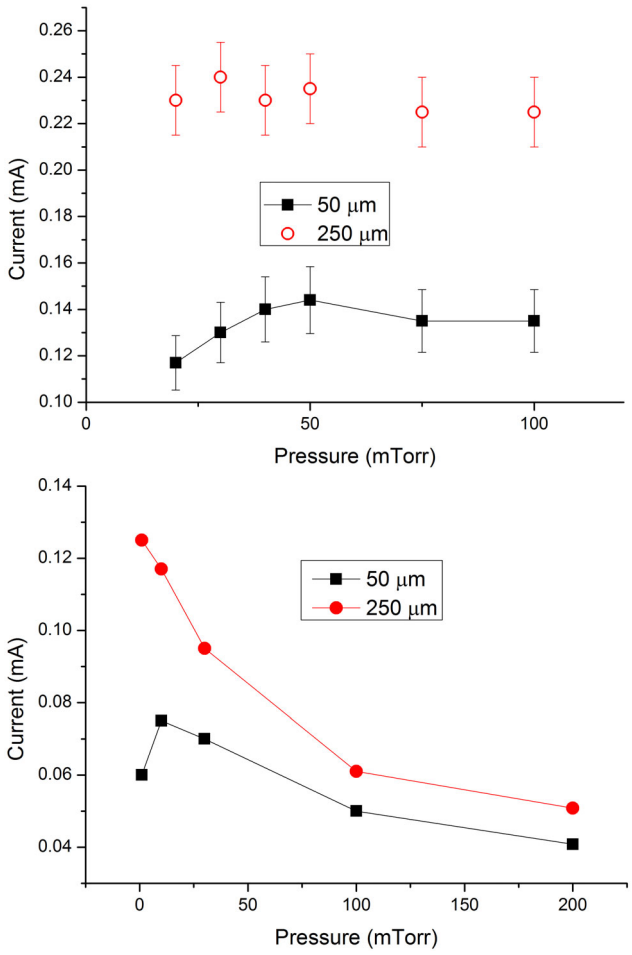

Fig. 10. Ion probe current as a function of neutral gas pressure. Results of Probe model for two probe radius 50 and 250 μm. (a) Experiment (fixed input power of 10 W). (b) Simulation (fixed plasma density 10^{10} cm^{-3}).

The absolute values of ion probe currents are presented in Figure 10 for two probe radii of 50 and 250 μm as functions of gas pressure. The experimental results in Figure 10a are shown for a fixed input discharge power of $P = 10$ W. The general effect of ion collisions is the probe current decrease due to the collisional "drag force". But it is also seen for 50 μm probe that the addition of a small amount of ion collisions leads to the increase of ion probe current due to the destruction of the ion orbital motion. This effect was discussed earlier in reference [14]. But for the typical RF CCP discharge conditions this non-monotonic behavior of the experimental probe current is shown for the first time. The results of numerical simulation are shown in Figure 10b for a fixed plasma density of $N_0 = 10^{10}$ cm^{-3}. As the plasma density increases with pressure for the fixed input power value, the experimental probe current in Figure 10 does not decrease with pressure as much as in simulation, where the plasma density value is kept constant.

In Figure 11, dependence of plasma density on input power obtained from experimental data and Probe model

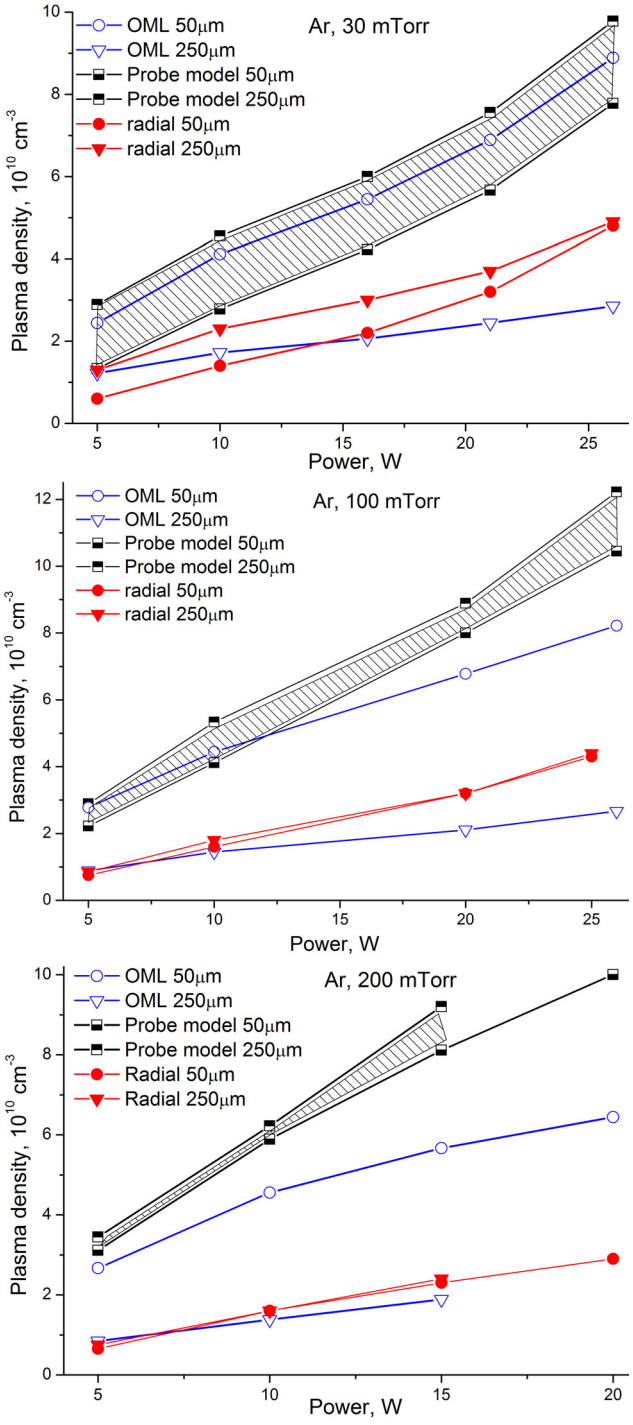

Fig. 11. Plasma density as a function of input power for various pressure –30, 100, 200 mTorr. Comparison of different approaches to ion probe current treatment.

simulation are shown for different argon pressure. Besides data processed with different collisionless analytical theories (OML and radial ion motion models) are presented in Figure 11 also.

The dashed area in Figure 11 shows the uncertainty in our numerical calculations, which provide the slightly different values of plasma density for two different probe radii. This uncertainty is discussed in the end of Section 3 and it almost disappears with pressure and does not disturb the results related to the collision effects. As expected, the collisionless theories underestimate the plasma density with pressure increase. It is clearly seen in case of $p = 200$ mTorr. However, the results of OML theory for thin probe at $p = 30$ mTorr correlate with the results of the numerical probe model due to the previously discussed collision effects. These effects (the destruction of orbital motion and "collision drag-force") could neutralize each other only in the specific range of discharge parameters. It would be erroneous conclusion to estimate the plasma density by using the simple formula (1) in a broad range of discharge parameters. In general with further pressure increase, the discrepancy in plasma density will be enhanced and the ion collisions should be taken into account. With the available computational resources the developed numerical probe model allows near the real time I-V curve interpretation and could be used for the plasma density calculation or for preliminary test of analytical models for various discharge parameters and gases.

5 Conclusions

The kinetic numerical Probe model was developed to determine plasma densities from the measured I-V curves and to reveal the role of ion collisions at a wide range of gas pressures and input powers. For this purpose the kinetic simulation of Ar^+ ion motion in Ar along with the experimental measurements of I-V probe characteristics are presented for typical plasma processing conditions. The experimental measurements of I-V curve for two cylindrical probes with radii of 50 and 250 μm in RF CCP argon discharge were performed at pressures of 30, 100 and 200 mTorr and input power of 5–30 W. The model computations are quite fast and can be used to precalculate data for further real time I-V curve analysis in the experimental probe measurements. Probe model uses experimental values of electron temperature and plasma potential as input parameters. The sensitivity of the model to these input parameters is discussed. Correctness of the used assumptions is tested in the PIC MCC discharge simulation. Plasma density values as a function of discharge input power are obtained from the developed Probe model for the pressure range of 30–200 mTorr.

The results of analytical collisionless theories of orbital and radial motion were compared with the results of numerical simulation with the Probe model to test the usage of these analytical theories beyond the formal scope of their applicability. It was shown that the collisionless theories commonly used for estimation of plasma density could underestimate the plasma density due to not taking into account the ion collision effects. For low pressure, the observed agreement of the plasma density values obtained from the collisionless OML theory (for the thin, 50 μm, probe) with the results of numerical Probe model is just a particular case of the conditions under study. Two opposite effects of ion collisions (the destruction of orbital motion and "collision drag-force") are partially

neutralize each other in case of an argon pressure of 30 and 100 mTorr. But this neutralization can not be a reliable basis for the use of OML theory at any particular plasma and probes parameters. Moreover, the collisionless theories are hardly applicable for higher pressures (>150–200 mTorr) where ion collisions should be taken into account. The relevant study and similar applicability analysis are needed for different background gases to avoid the possible mistakes in the plasma density derivation by using of any simple theory.

Our practical recommendation is to use kinetic numerical models for the correct interpretation of the ion part of experimental I-V curve. With the available computational resources and the development of many kinetic codes [31], this is quite possible to implement.

This work will be extended further on the different noble and molecular gases as a part of plasma diagnostics tool for various discharges and plasma conditions.

This research was supported by the Russian Science Foundation Grant 14-12-01012.

References

1. N. Fox-Lyon, A.J. Knoll, J. Franek, V. Demidov, V. Godyak, M. Koepke, G.S. Oehrlein, J. Phys. D **46**, 485202 (2013)
2. K. Kurchikov, A. Kovalev, A. Vasilieva, O. Braginsky, Bull. Am. Phys. Soc. **58**, 60 (2013)
3. J.B. Boffard, R.O. Jung, C.C. Lin, A.E. Wendt, Plasma Sources Sci. Technol. **19**, 065001 (2010)
4. D.L. Crintea et al., J. Phys. D **42**, 045208 (2009)
5. V.A. Godyak, R.B. Piejak, B.M. Alexandrovich, Plasma Sources Sci. Technol. **1**, 36 (1992)
6. V.A. Godyak, V.I. Demidov, J. Phys. D **44**, 233001 (2011)
7. L. Oksuz, F. Soberon, A.R. Ellingboe, J. Appl. Phys. **99**, 013304 (2006)
8. H. Mott-Smith, I. Langmuir, Phys. Rev. **28**, 727 (1926)
9. I.B. Bernstein, I.N. Rabinowitz, Phys. Fluids **2**, 112 (1959)
10. J.G. Laframboise, University Toronto Inst. Aerospace Studies Report No. 100, 1966
11. J.E. Allen, R.L.F. Boyd, P. Reynolds, Proc. Phys. Soc. London B **70**, 297 (1957)
12. Y.S. Chou, L. Talbot, D.R. Willis, Phys. Fluids **9**, 2150 (1966)
13. L. Talbot, Y.S. Chou, in *Rarefied Gas Dynamics* (Academic Press, New York, 1966), p. 1723
14. Z. Zakrzewski, T. Kopiczyñski, Plasma Phys. **16**, 1195 (1974)
15. M. Tichy, M. Sicha, P. David, T. David, Contrib. Plasma Phys. **34**, 59 (1994)
16. C.H. Shih, E. Levi, AIAA **9**, 1673 (1971)
17. http://www.hidenanalytical.com, Plasma Diagnostics – Plasma Characterisation Using a Langmiur Probe by Hiden Analytical
18. F.F. Chen, J.D. Evans, W. Zawalski, Plasma Sources Sci. Technol. **21**, 055002 (2012)
19. D. Trunec, P. Spanel, D. Smith, Contrib. Plasma Phys. **42**, 91 (2002)
20. F. Taccogna, S. Longo, M. Capitelli, Eur. Phys. J. Appl. Phys. **22**, 29 (2003)
21. A. Cenian, A. Chernukho, A. Bogaerts, R. Gijbels, C. Leys, J. Appl. Phys. **97**, 123310 (2005)
22. F. Iza, J.K. Lee, J. Vac. Sci. Technol. A **24**, 1366 (2006)
23. T. Kopiczynski, DSc. thesis, Institute of Fluid Flow Machines, Gdansk, 1977
24. C.M. Horwitz, J. Vac. Sci. Technol. A **1**, 1795 (1983)
25. V.A. Godyak, R.B. Piejak, J. Vac. Sci. Technol. A **8**, 3833 (1990)
26. T.V. Rakhimova et al., IEEE Trans. Plasma Sci. **35**, 1229 (2007)
27. A.V. Phelps, J. Appl. Phys. **76**, 747 (1994)
28. http://jila.colorado.edu/∼avp/collision_data/electron-neutral/ELECTRON.TXT
29. J.W. Eastwood, R.W. Hockney, *Computer Simulation using Particles* (McGraw-Hill, New York, 1981)
30. V.V. Ivanov, O.V. Proshina, T.V. Rakhimova, A.T. Rakhimov, D. Herrebout, A. Bogaerts, J. Appl. Phys. **91**, 6296 (2002)
31. M.M. Turner et al., Phys. Plasmas **20**, 013507 (2013)